Electronic Supporting Information

Aggregation-Induced Emission Enhancement and Reversible Mechanochromic Luminescence of Quinoline-Based Zinc(II) Schiff Base Complexes

Di Qiao,[a,b] Jin-Yun Wang,[a] Li-Yi Zhang,[a] Feng-Rong Dai,*[a] and Zhong-Ning Chen*[a,b]

[a] State Key Laboratory of Structural Chemistry, Fujian Institute of Research on the Structure of Matter, Chinese Academy of Sciences, Fuzhou, Fujian 350002, China

[b] College of Chemistry and Materials Science, Fujian Normal University, Fuzhou 350007, China

*To whom correspondence should be addressed. E-mail: dfr@fjirsm.ac.cn, czn@fjirsm.ac.cn; Tel: (+86) 591-6317-3171

Table S1. Crystallographic Data for Complexes **1–3**.

	1	**2**	**3**
empirical formula	$C_{36}H_{28}F_6N_4O_8S_2Zn$	$C_{38}H_{32}F_6N_4O_{10}S_2Zn$	$C_{40}H_{34}F_6N_4O_{10}S_2Zn$
formula weight	888.11	948.16	974.2
crystal system	monoclinic	triclinic	monoclinic
space group	*P*2/c	*P*-1	*C*2/c
a (Å)	21.4502(17)	13.802(2)	27.506(3)
b (Å)	10.4993(7)	14.659(2)	10.9018(12)
c (Å)	18.7583(14)	19.964(4)	18.564(2)
α (°)	90	87.244(6)	90
β (°)	114.568(2)	86.516(6)	130.821(4)
γ (°)	90	89.582(6)	90
V (Å^3)	3842.1(5)	4027.1(12)	4212.6(8)
Z	4	4	4
D(calcd) (g cm^{-3})	1.535	1.564	1.536
μ (Mo K_α) (mm^{-1})	0.833	0.804	0.771
F(000)	1808	1936.0	1992.0
θ range (°)	2.278 – 24.997	2.338 – 25.352	2.899 – 37.907
reflections collected / unique	48355 / 6760 [R_{int} = 0.1144]	86157 / 14701 [R_{int} = 0.0438]	66552 / 10037 [R_{int} = 0.1370]
data / restraints / parameters	6760 / 502 / 515	14701 / 185 / 1180	10037 / 0 / 285
GOF	1.039	1.084	1.036
R_1 (I>2σ(I))	0.0479	0.0487	0.0606
wR_2 (I>2σ(I))	0.1262	0.1162	0.1796
R_1 (all data)	0.0766	0.0568	0.0796
wR_2 (all data)	0.1623	0.1204	0.1946
$\Delta\rho$ / e A$^{\circ -3}$	0.549, -0.733	0.786, -0.644	0.877, -1.225

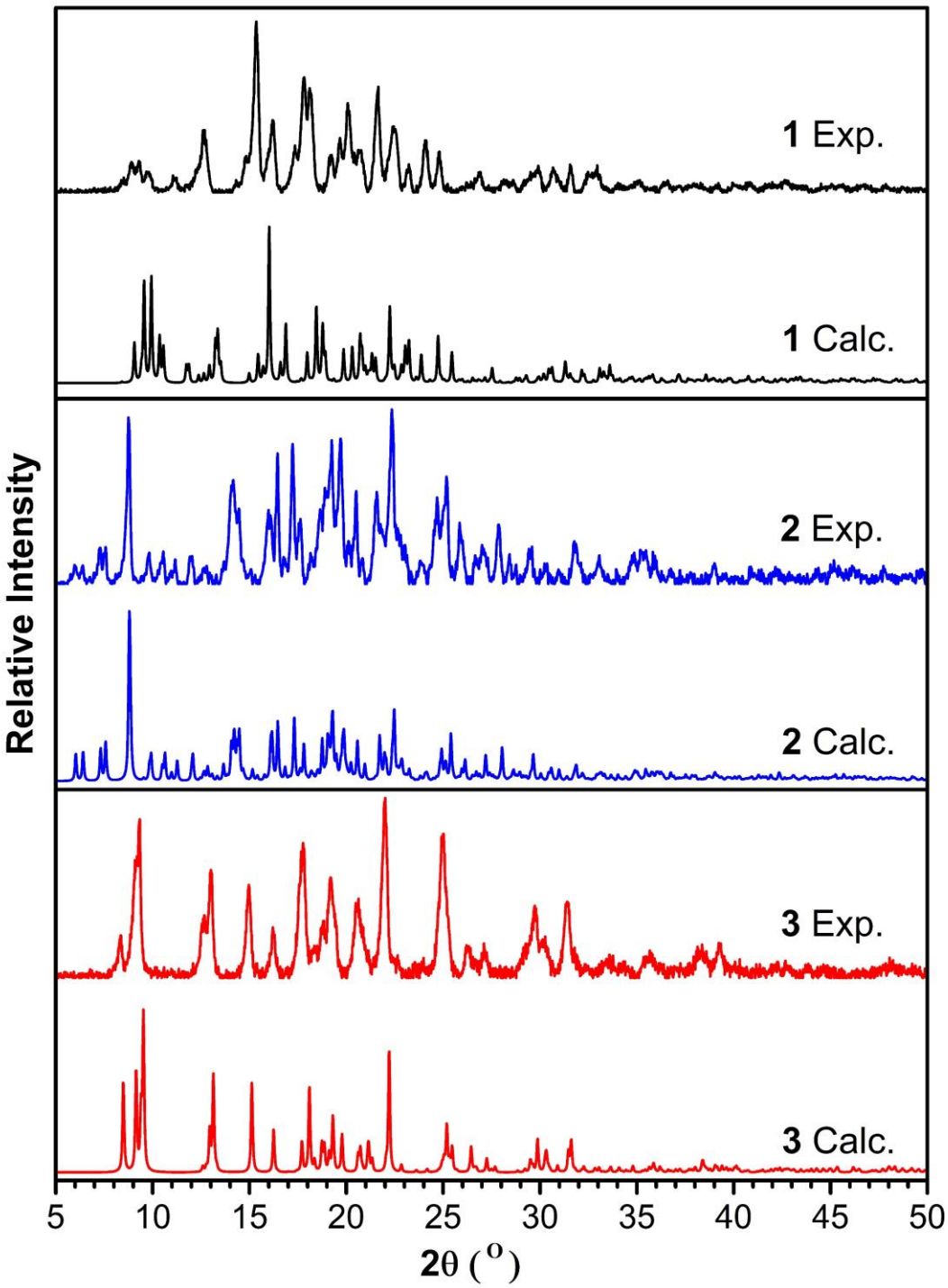

Fig. S1. Experimental PXRD patterns of complexes **1–3** in comparison with simulated patterns calculated from single-crystal structures.

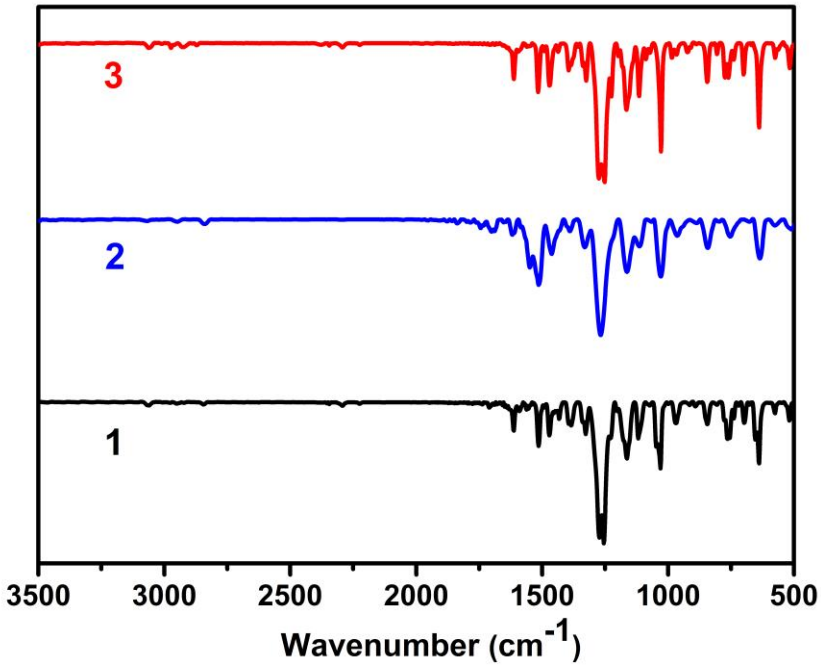

Fig. S2. FT-IR spectra of complexes **1–3**.

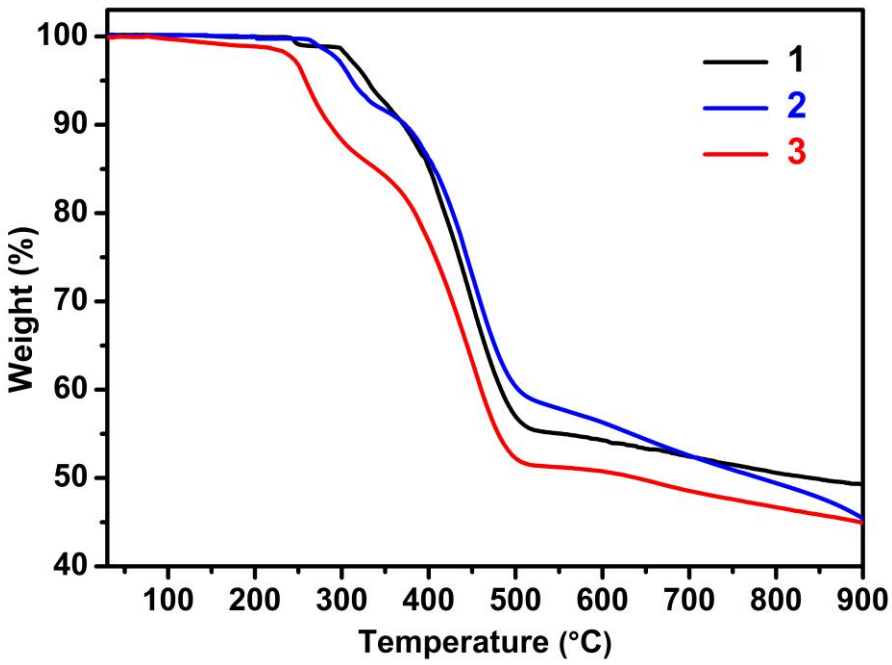

Fig. S3. TGA plots of complexes **1–3**.

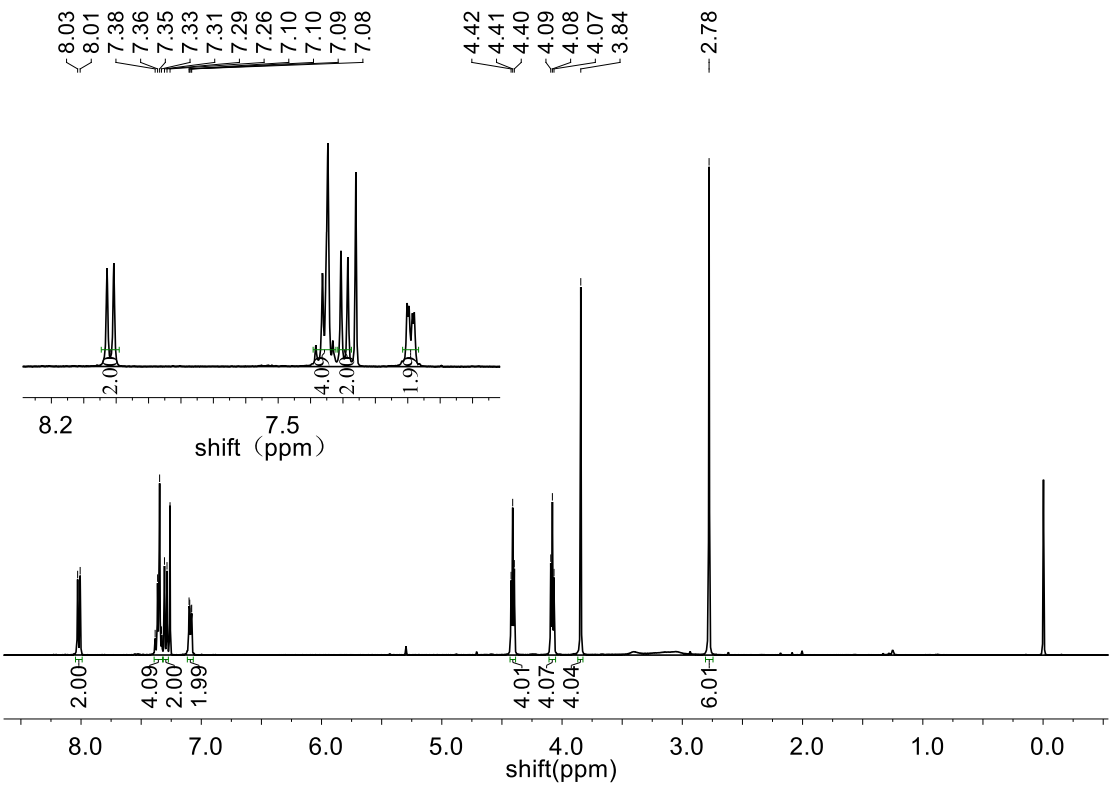

Fig. S4. ^{1}H NMR spectrum of 1, 2-bis(2-((2-methyl-quinolin-8-yl)oxy)ethoxy)-ethane in $CDCl_3$.

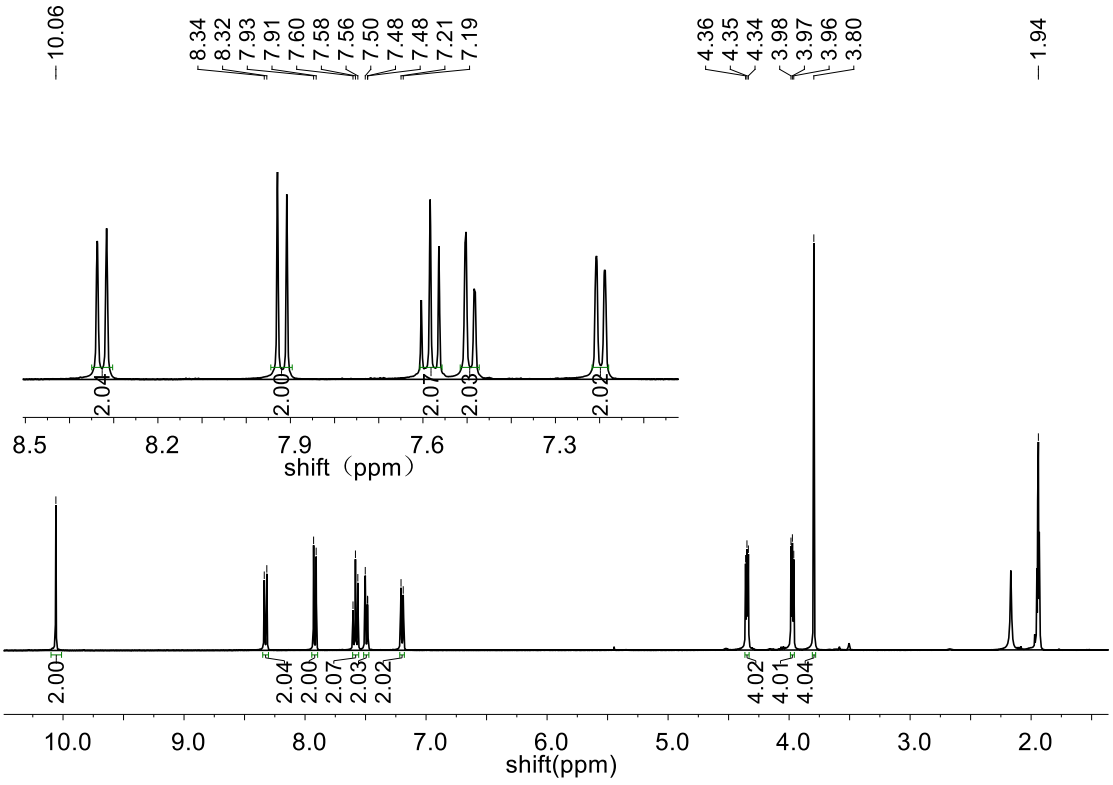

Fig. S5. ^{1}H NMR spectrum of **L2** in CD_3CN.

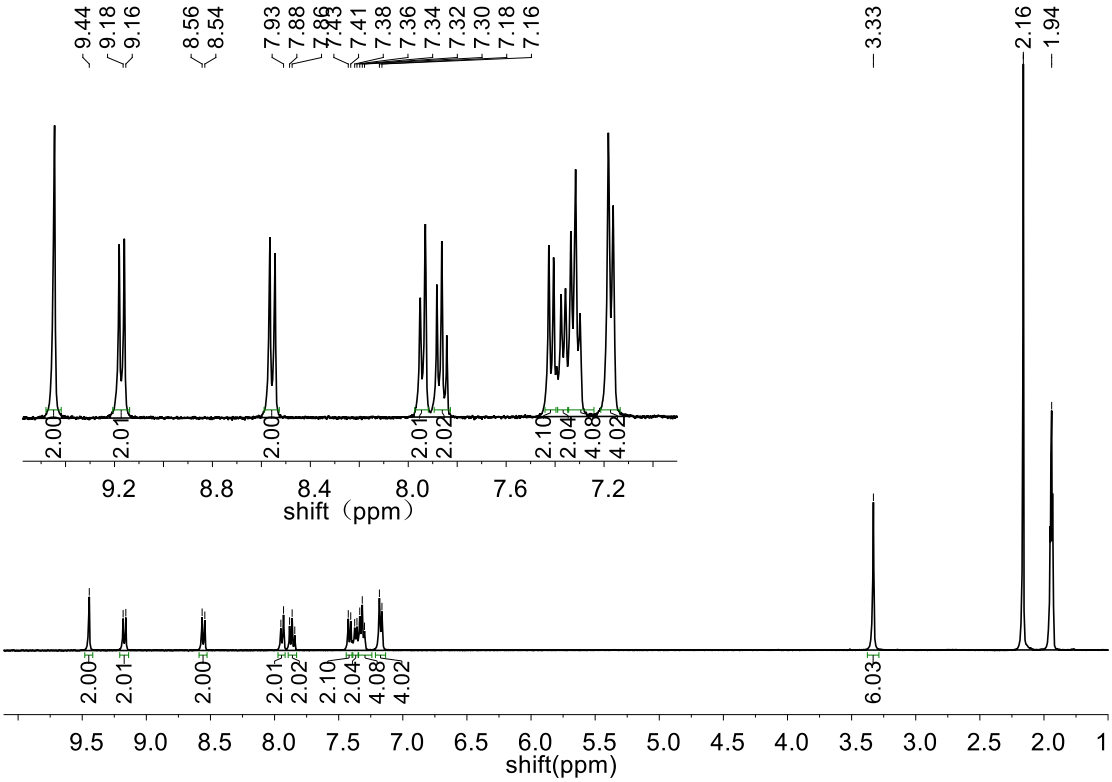

Fig. S6. ^{1}H NMR spectrum of complex **1** in CD_3CN.

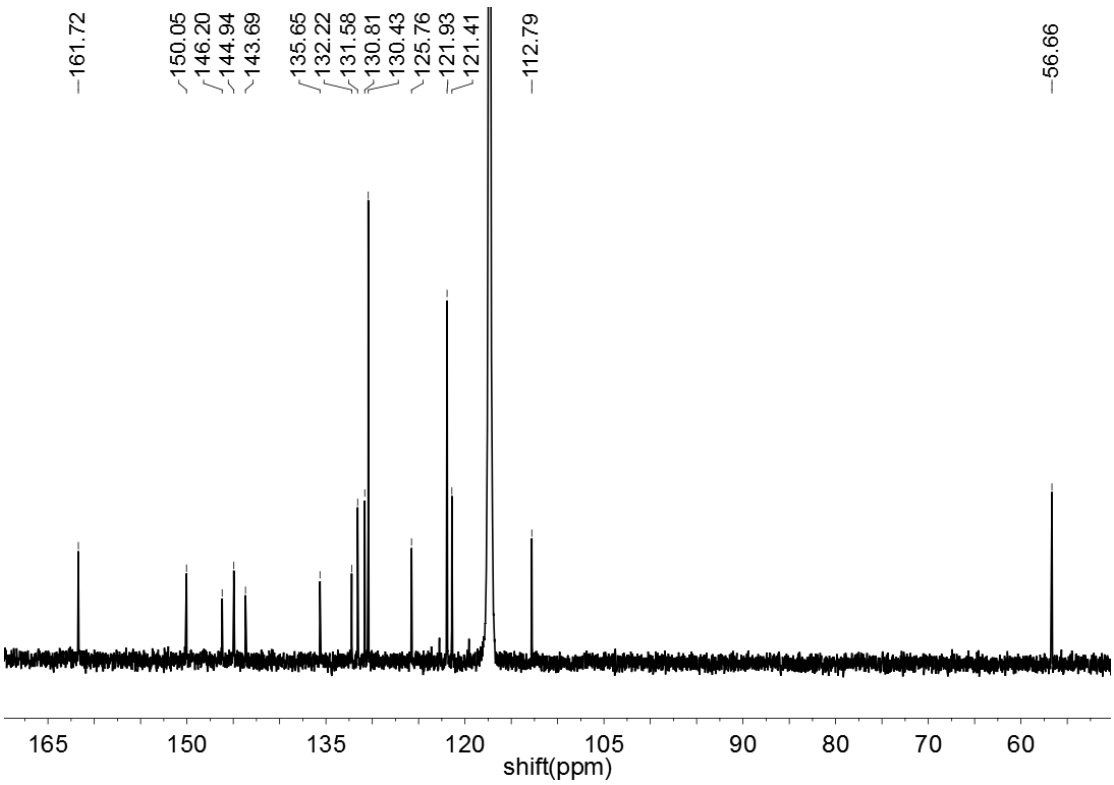

Fig. S7. ^{13}C NMR spectrum of complex **1** in CD_3CN.

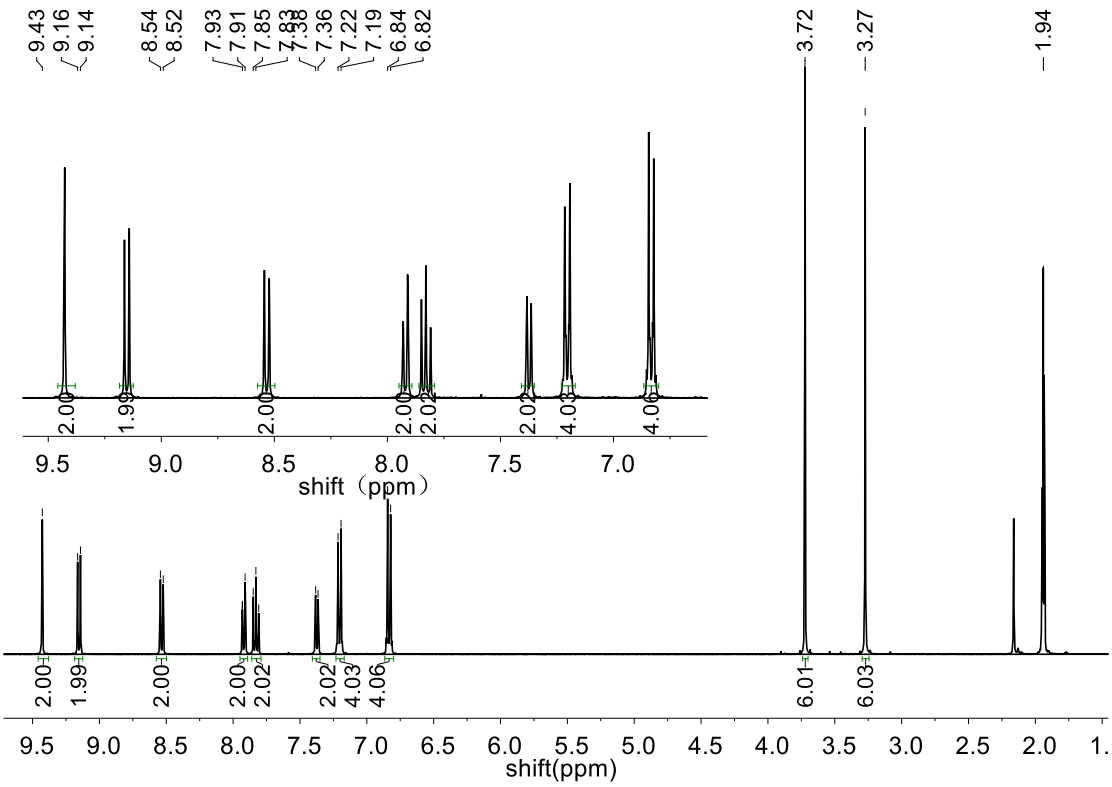

Fig. S8. ^{1}H NMR spectrum of complex **2** in CD_3CN.

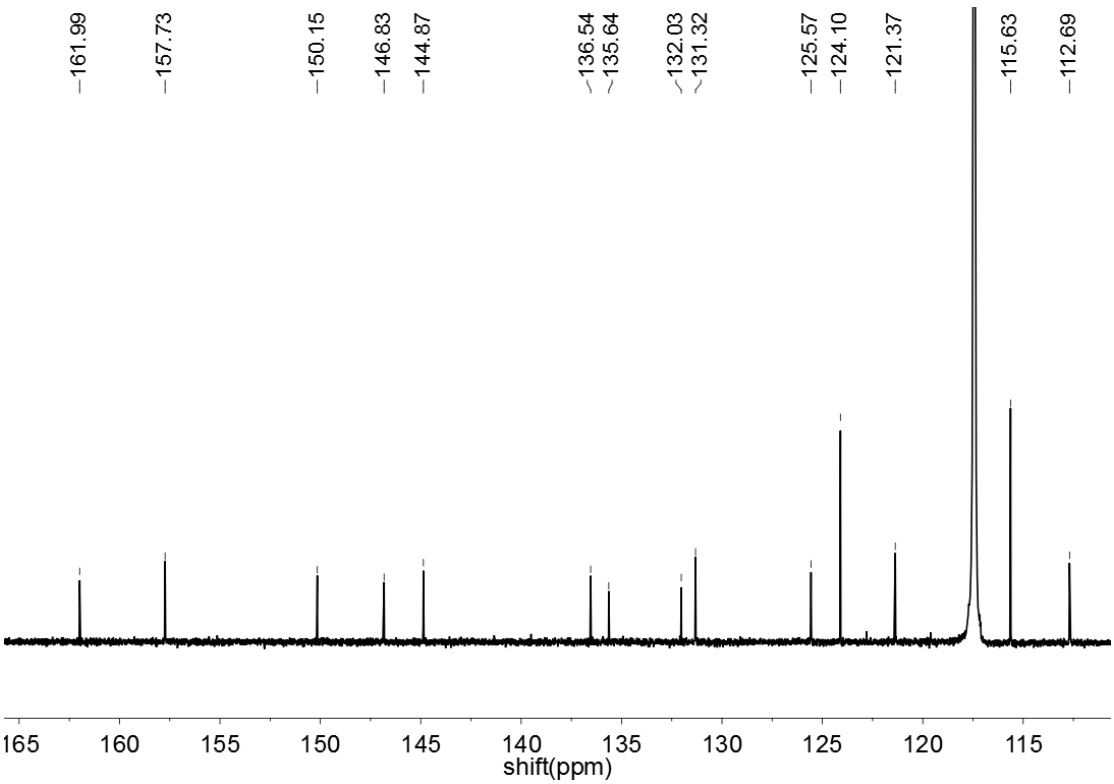

Fig. S9. ^{13}C NMR spectrum of complex **2** in CD_3CN.

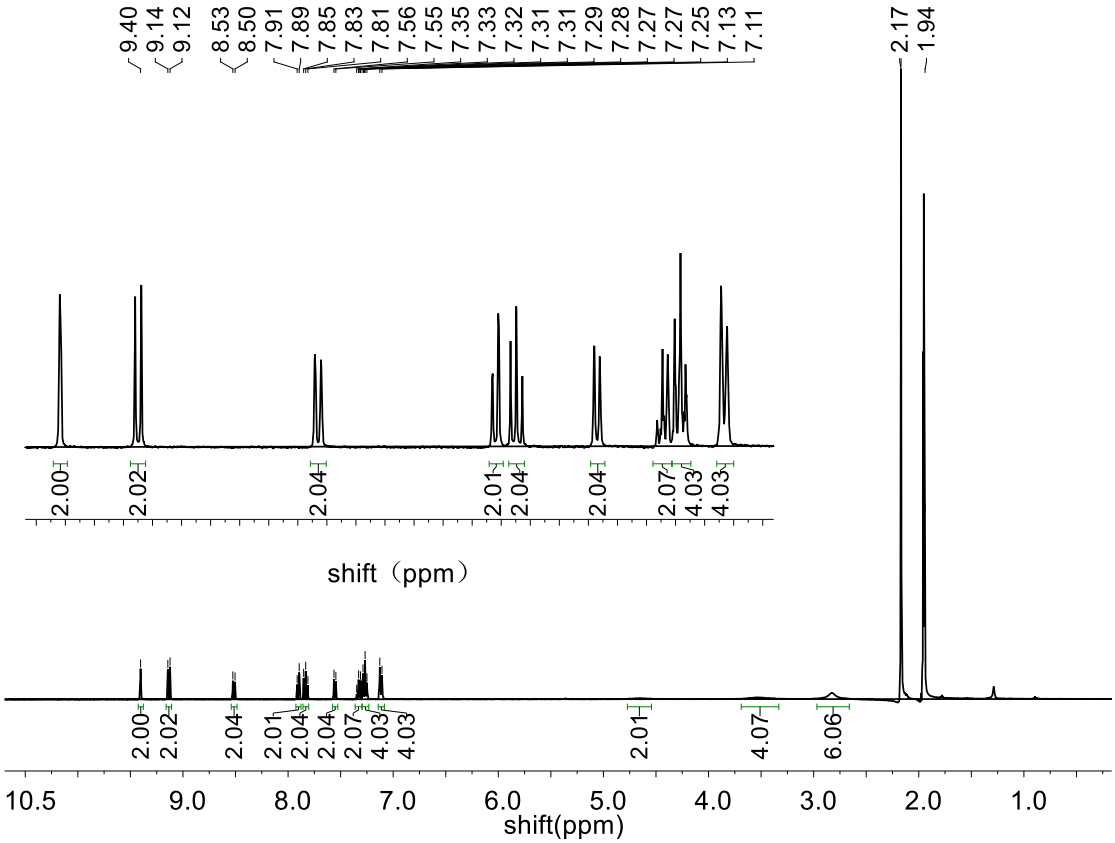

Fig. S10. ^{1}H NMR spectrum of complex **3** in CD_3CN.

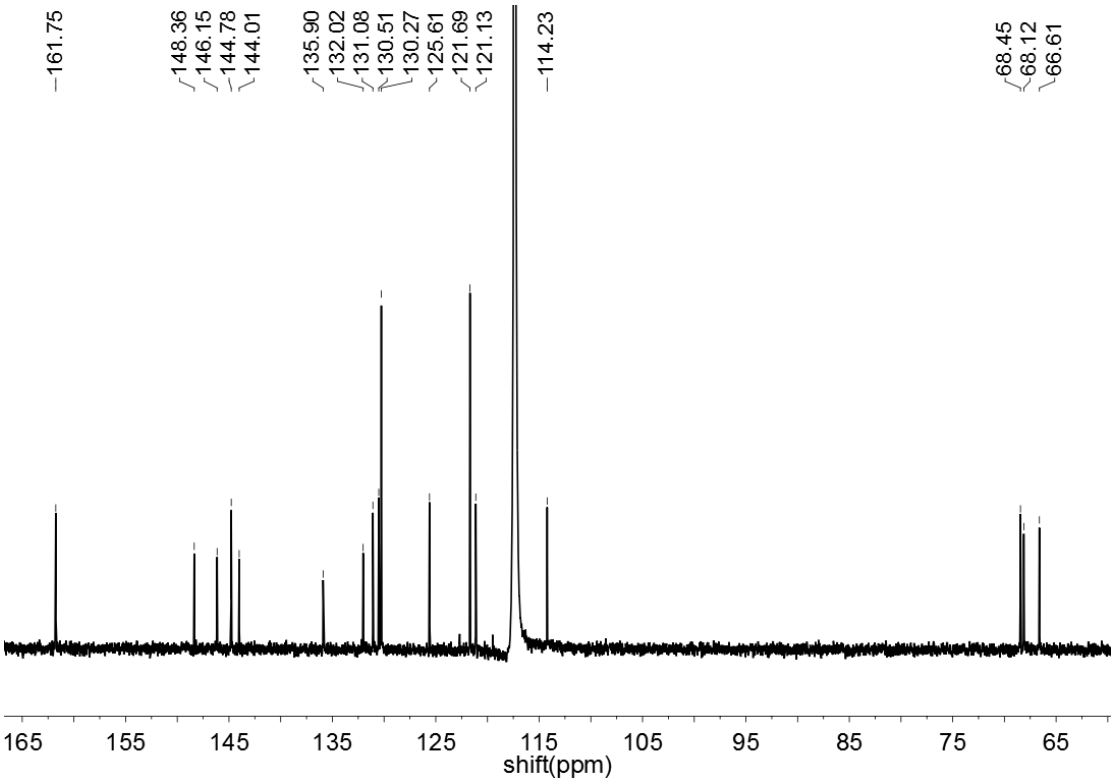

Fig. S11. ^{13}C NMR spectrum of complex **3** in CD_3CN.

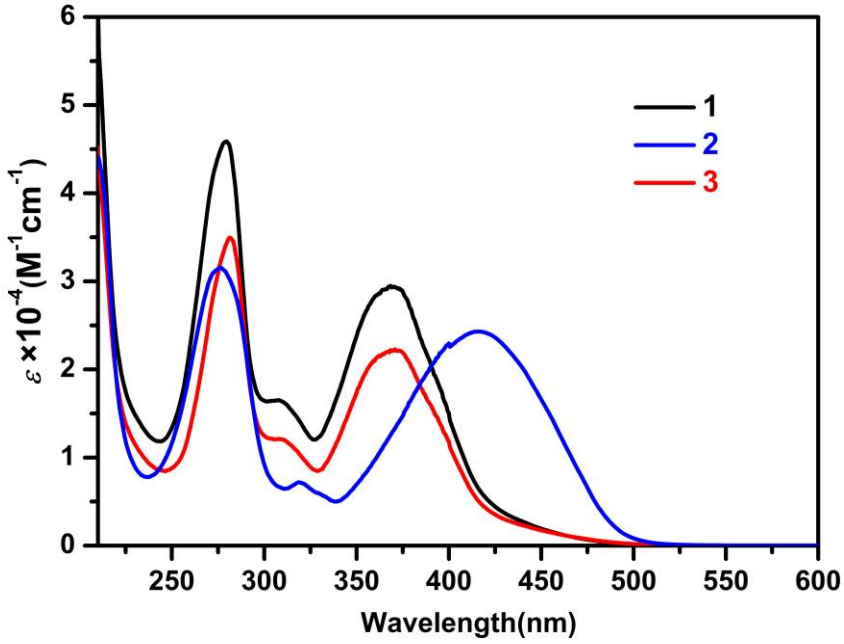

Fig. S12. UV-Vis absorption spectra of complexes **1**–**3** in acetonitrile solutions.

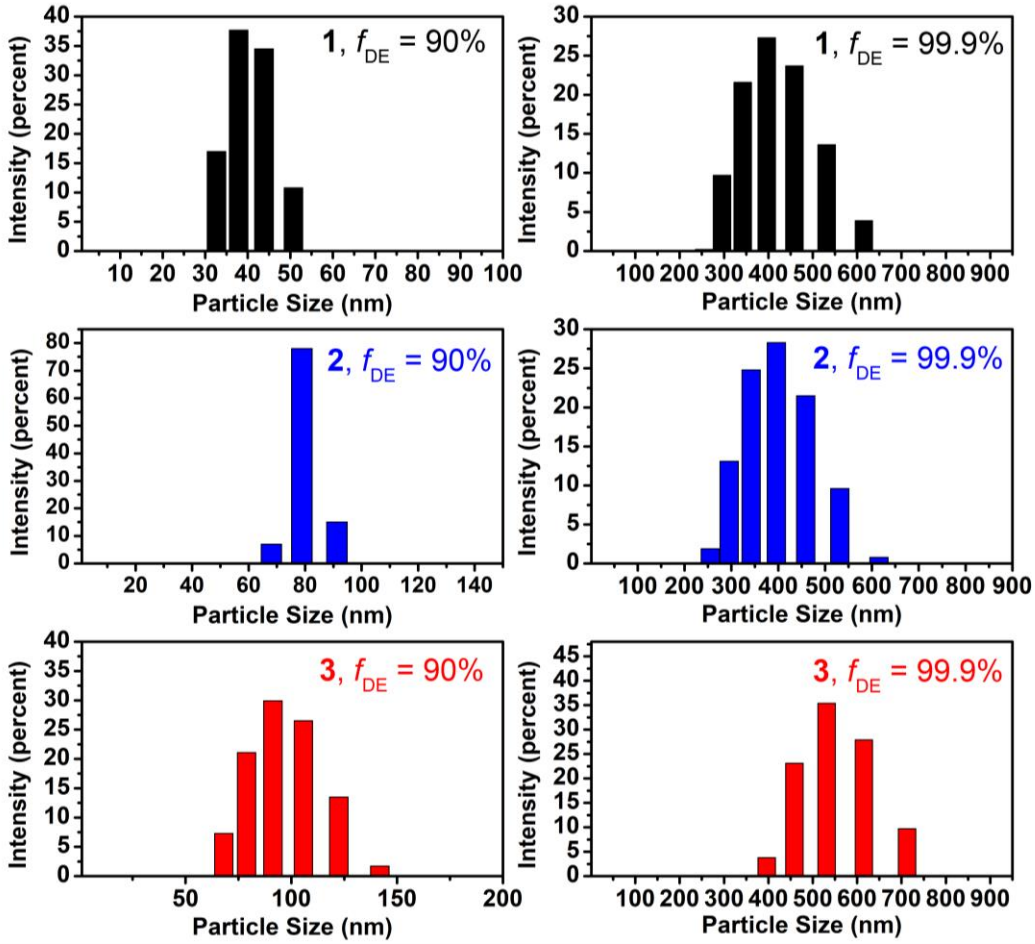

Fig. S13. Particle size distributions of complexes **1**–**3** (25 μM) in Et_2O/CH_3CN mixture with different Et_2O fractions, indicating the formation of nano-aggregated

phases.

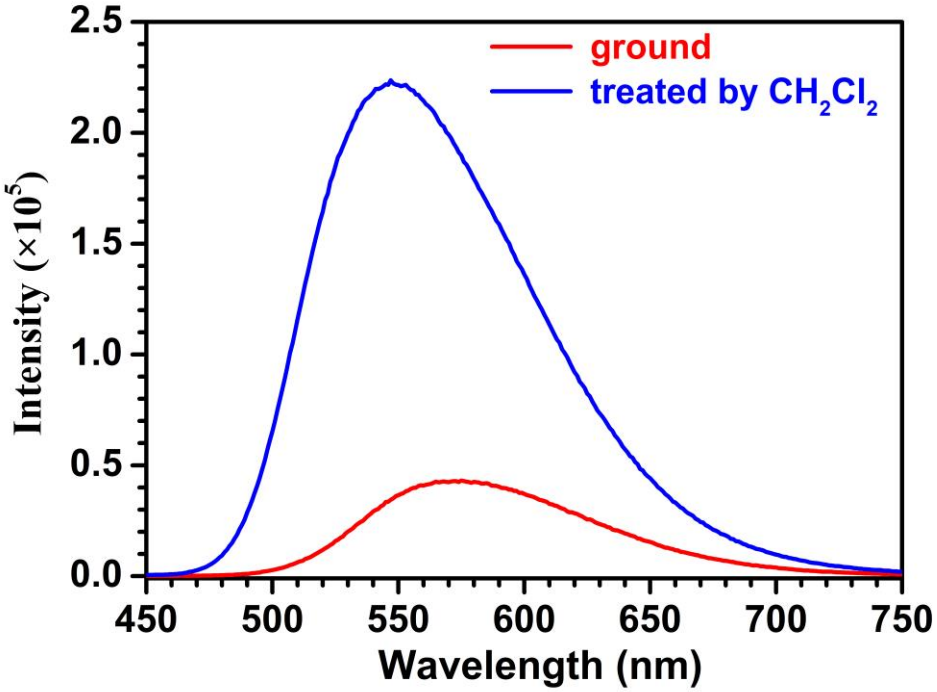

Fig. S14. Emission spectra of complex **1** during the grinding-fuming cycle.

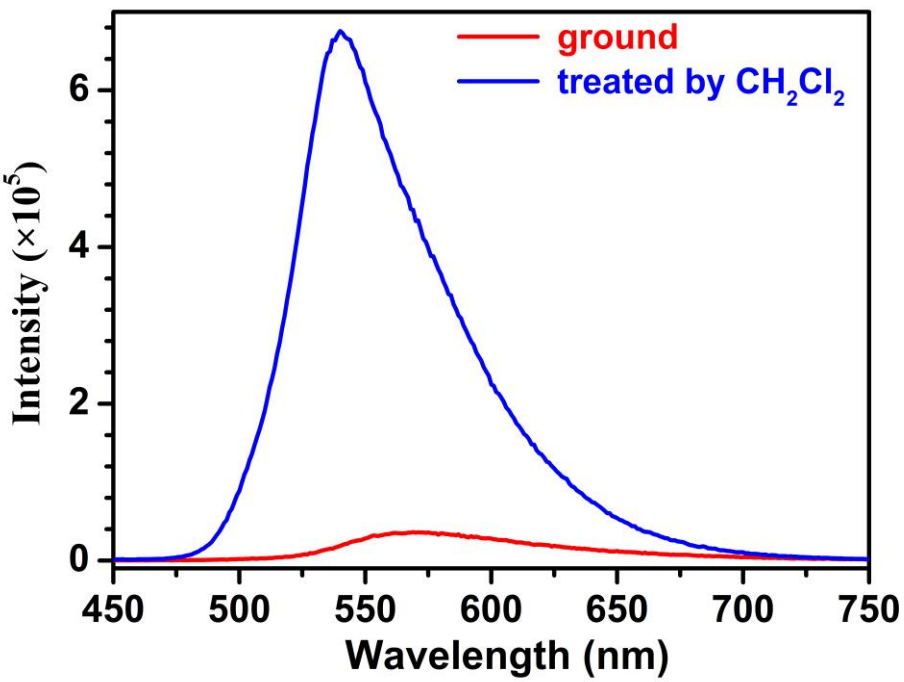

Fig. S15. Emission spectra of complex **2** during the grinding-fuming cycle.

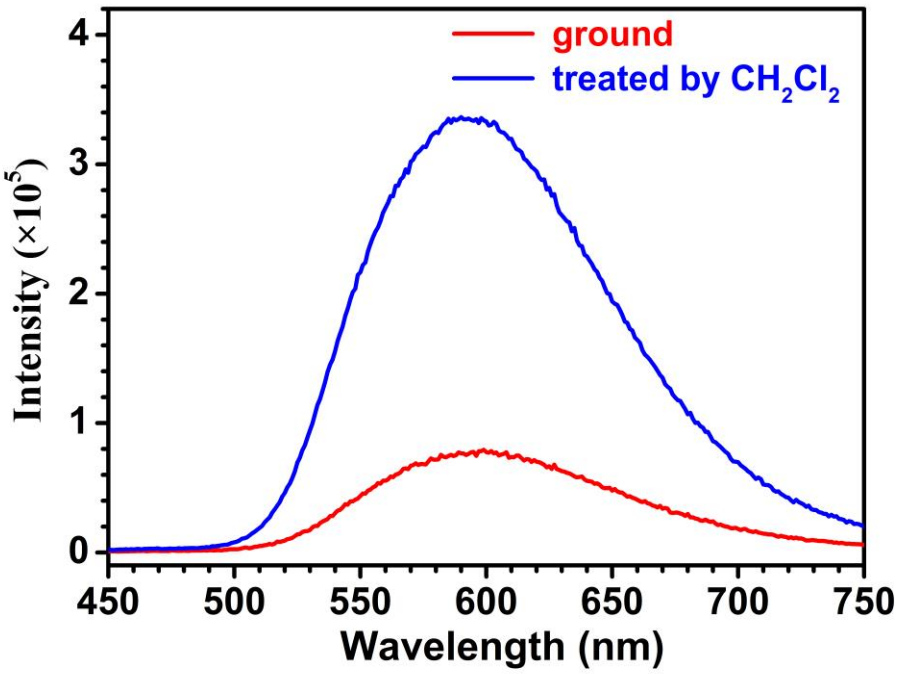

Fig. S16. Emission spectra of complex **3** during the grinding-fuming cycle.

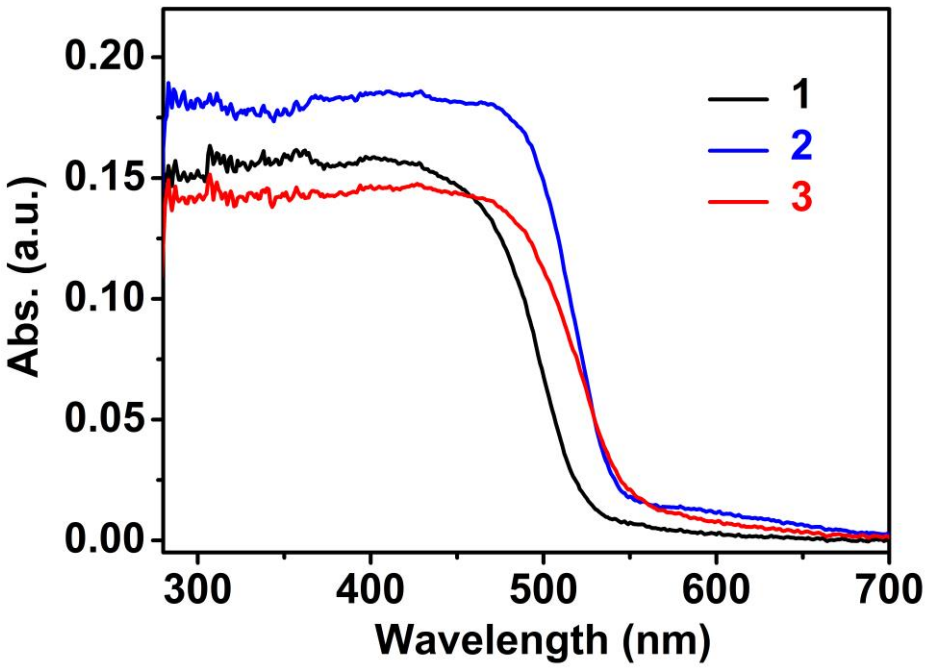

Fig. S17. UV-Vis spectra of complexes **1**–**3** in solid state.